Journal of Bioscience and Bioengineering
VOL. 127 No. 6, 767–773, 2019

www.elsevier.com/locate/jbiosc

ELSEVIER

Bio-ionic liquid pretreatment and ultrasound-promoted enzymatic hydrolysis of black soybean okara

Cheng-An Yu and Chun-Yao Yang*

Department of Food Science, Fu Jen Catholic University, No. 510, Zhongzheng Rd., Xinzhuang Dist., New Taipei City 24205, Taiwan, ROC

Received 18 September 2018; accepted 16 December 2018
Available online 9 January 2019

The effective processing method to produce fermentable sugars and modify the microstructure of black soybean okara using bio-ionic liquid (bio-IL) pretreatment and ultrasound-promoted enzymatic hydrolysis was investigated. The morphology and structural characteristics of okara before and after bio-IL pretreatment and enzymatic hydrolysis under different ultrasonic frequencies were analyzed by field emission scanning electron microscope (FE-SEM), X-ray energy dispersive spectrometer (EDS), and Fourier transform infrared spectroscopy (FTIR). Without pretreatment, the production of total reducing sugar (TRS) under ultrasound (40 kHz/300 W) was 3.4 times of that without ultrasound. Using the bio-IL choline acetate ([Ch][OAc]) in water for the pretreatment of black soybean okara, the TRS production of enzymatic hydrolysis was further increased to 5.2 times of that without ultrasound in 4 h of reaction. The analysis by FTIR and EDS showed that the highly structured matrix of okara was unfolded and broken by the action of combining ultrasound and choline acetate pretreatment, due to which the surface structures with large pores were presented to facilitate the reduction of unfavorable hindrance for enzymatic hydrolysis. The simplified kinetic model was proposed to describe the transport and reaction phenomena of enzymes in a solid–liquid system by using two kinetic parameters to show the impeded behavior of enzyme within the matrix of okara. The combination of bio-IL pretreatment and ultrasound-promoted enzymatic hydrolysis was able to make the efficient structural changes of black soybean okara to enhance the digestion of enzymes, and the okara could be valorized for use in foods.

[**Key words:** Okara; Ultrasound; Bio-ionic liquid; Enzymatic hydrolysis; Hydrolysis kinetics]

Soybean (*Glycine max* (L.) Merr.) is rich in nutrients, such as protein, carbohydrates, fiber, vitamins, minerals, with the structure interlaced by cellulose, protein and lipid. Black soybean is the soybean rich in anthocyanins with black seed coat, and is often used for detoxification and anti-inflammatory in traditional Chinese medicine (1,2). Okara is the side-product in the manufacturing processes of soymilk or tofu from soybean with the production of about 1.1–1.2 kg from each kilogram of soybean in the tofu processes. Each year, the production of okara by the tofu-manufacturing industry is about 800,000 tons in Japan, 310,000 tons in Korea, and 2,800,000 tons in China (3).

Generally, okara contains about 15.2–33.4 % of protein, 42.4–58.1 % of dietary fiber, 3.8–5.3 % of carbohydrates, and 3.0–4.5 % of ash in weight, and lacks fermentable carbohydrates for efficient microbial growth in okara (3). Okara can be directly used in food in some areas (4), but its consumption is far less than its production. Most of the okara is often mixed in animal feed, discarded directly (5), used as compost (6), or incinerated (4). As a by-product in soybean processing, okara contains useful ingredients that are beneficial to human health and is worth reusing. Various processing procedures on okara can affect the nutrient compositions and the bioactivity. The valorization of okara depends on the method of processing, and enzymatic hydrolysis to produce fermentable sugars is one way to utilize okara with high added-values (7,8).

Due to the solid type of okara, the enzymatic hydrolysis is usually affected by the accessibility of enzyme to the insoluble substrate, leading to the low reaction rate. In such enzymatic reactions in a heterogeneous system, the overall reaction rate is subjected to several factors, including transport resistances of enzymes, adsorption of enzymes on inert sites, and product inhibition, causing the effective enzymes quickly diminished to decline the reaction rate dramatically (9–11). The accessibility of enzymes into solid substrates is limited by the obstacles hindering the diffusion of enzymes to reach the reaction sites of substrates. Ultrasonic irradiation as a non-thermal green technology has attracted increasing attention in food processing, such as extraction, microbial fermentation, emulsification, filtration, and tenderization (12,13). Ultrasonic irradiation can generate cavities in liquid phase by violent collapse of bubbles and local hotspots to promote chemical reactions (14–16), such that it can be employed to promote the transport and reaction of enzymes within the network structure of solid substrate.

Moreover, the pretreatment on the substrate using appropriate compounds can usually improve the accessibility of enzymes at the reaction site. The ILs are considered to be a green solvent having been widely applied in separation, catalysis, biotechnology, coatings and nanomaterials (17,18). However, the ILs used in biotechnology are somewhat limited by the considerations of toxicological, ecological and economic constraints (19). The new generation of ILs

---

* Corresponding author. Tel.: +886 2 29053624; fax: +886 2 22093271.
E-mail address: 133810@mail.fju.edu.tw (C.-Y. Yang).

1389-1723/$ – see front matter © 2018, The Society for Biotechnology, Japan. All rights reserved.
https://doi.org/10.1016/j.jbiosc.2018.12.007

that are derived from naturally occurring bases (e.g., choline) and acids (e.g., amino acids) is regarded as bio-ILs, among which the choline based ILs are classified as bio-distributed molecules having many biological functions (20) and present the potential application in biotechnology.

The okara contains proteins, dietary fiber and valuable compounds for reuse; however, the high content of fibers in okara and unsavory texture for eating have made it difficult to be used (21). Besides, the highly structured fibers also make the digestion of okara very difficult when using enzymes for a very long reaction time (21). Thus, the modification of okara structure is advantageous to valorize the use of okara in foods. An efficient processing method at mild conditions to modify the microstructure and reduce the content of fibers accompanying with the production of fermentable sugars would be beneficial for the utilization of okara. In addition, the use of IL with good biocompatibility is essential when applied in the biomaterials relating to the food use. Choline, as an additive in human nutrition and animal feed, is expected to be biodegradable with non-toxicity, and [Ch][OAc] is a choline-derived IL showing the property of dissolving some extents of microcrystalline cellulose (22,23). Thus, [Ch][OAc] as a bio-IL is suitable to be used for the pretreatment of biomaterials. In this study, the aim was to develop the effective method to produce reducing sugars and modify the highly structured matrix of black soybean okara by using bio-IL [Ch][OAc] pretreatment under sonication and ultrasound-promoted enzymatic hydrolysis with cellulase. The structure changes and characterization of okara before and after bio-IL pretreatment as well as enzymatic hydrolysis with or without ultrasound were analyzed. A simplified kinetic model for this solid−liquid system was proposed by considering the impeded behavior of enzymes within the network structure of okara using two kinetic parameters to describe the enzymatic hydrolysis reaction.

MATERIALS AND METHODS

Materials and ultrasonic systems The okara was prepared from the Tainan No. 3 black soybean, *G. max* (L.) Merr., which was purchased from Shia Ying Farmers' Associations in Tainan County, Taiwan. The enzyme used for hydrolysis was the cellulase from *Trichoderma reesei* (EC Number 232-734-4, ≥700 endoglucanase units (EGU)/g, from Sigma−Aldrich), and the bio-IL used for pretreatment of okara was [Ch][OAc] (≥95.0%, from Sigma−Aldrich). Other chemicals were purchased from Sigma (St. Louis, MO, USA), Merck (Darmstadt, Germany), Avantor (Center Valley, PA, USA), and Honeywell Fluka (Morris Plains, NJ, USA). The pretreatment and enzymatic hydrolysis of okara powder were performed in thermostatically ultrasonic bath systems with 40 kHz/300 W or 120 kHz/300 W of ultrasound frequency/electric power (LEO-3002S, LEO-3002H, LEO Ultrasonic Co., Taiwan).

Preparation of black soybean okara The fresh black soybeans were rinsed to clean thoroughly, and subsequently soaked in distilled water at a ratio of soybeans to water being 1:6 (w/w) for overnight. After that, the black soybeans were separated, drained, and homogenized in distilled water at a ratio 1:10 (w/w) of soaked soybeans to water for 3 min. The black soymilk was filtrated to leave the fresh okara, which was then dried at 40 °C for 48 h. The dried okara was ground, screened through 60-mesh sieves and stored at −18 °C for use.

Component analysis of black soybean and okara The compositions of black soybeans and black soybean okara were analyzed for water, ash, crude protein, crude fat, and dietary fiber (Table S1). The methods used to determine the contents of water, crude fat, crude protein, and ash were in accordance with Chinese National Standards with a slight modification (24−27), and the content of dietary fiber was determined using AOAC Official Methods with a slight modification (28).

Pretreatment of okara with bio-IL choline acetate under ultrasound Using IL to pretreat biomass can modify the structure of biomass to get a high efficiency for utilization. For the environmentally friendly concern, the bio-IL [Ch][OAc] that dissolved in water or acetate buffer solution was employed to pretreat the okara under ultrasonic irradiation. The acetate buffer solution was prepared from acetic acid and sodium acetate solutions to make the acetate buffer solution at pH value of pH 5 ± 0.1. The bio-IL solution was prepared by adding 1 g of [Ch][OAc] into 50 mL of deionized water or acetate buffer solution in a round-bottom flask, in which 1 g of okara powder was added and treated at 60 °C under 40 kHz/300 W of ultrasound for 3 h. Then, the solid precipitate was obtained by centrifuging at 3800 rpm for 10 min. After that, the precipitate was washed with deionized water and centrifuged at 3800 rpm for 10 min, and this step was repeated at least three times to remove [Ch][OAc] and then freeze-dried to obtain the bio-IL pretreated okara. The recovery of pretreated okara was estimated using Eq. 1,

$$\text{Recovery of pretreated okara} = \frac{\text{Weight of dried okara after pretreatment}}{\text{Weight of okara before pretreatment}} \times 100\% \tag{1}$$

The results of okara recovery accompanying with the contents of crude protein and ash were determined for the okara treated at different ultrasonic conditions (Table S2).

Enzymatic hydrolysis of okara The enzymatic hydrolysis reaction of okara was conducted at 50 °C using cellulase solution without or with [Ch][OAc] pretreatment and ultrasonic irradiation at 40 kHz/300 W or 120 kHz/300 W. The cellulase solution (1.0 g/mL, ≥ 70 EGU/g) was prepared from 3 g of commercial cellulase (≥700 EGU/g) and 27 g of acetate buffer solution (pH 5 ± 0.1). The okara (100 mg) was mixed with 7-mL of the cellulase solution for enzymatic hydrolysis. At each sampling time (30, 60, 120, 180, and 240 min), the hydrolysis reaction was stopped, and the reaction solution was then heated by boiling water for 10 min to inactivate the enzyme. The reaction solution was centrifuged at 3800 rpm for 10 min to obtain the supernatant for the analysis of total reducing sugar (TRS) produced. The TRS was determined by using the 3,5-dinitrosalicylic acid (DNS) method (29) with a spectrophotometer (Hitachi Double-Beam Spectrophotometer UH5300, Hitachi, Tokyo, Japan). The TRS produced was calculated by Eq. 2:

$$\text{TRS production (mg/g}-\text{okara)} = \frac{\text{Weight (mg) of TRS produced}}{\text{Weight (g) of dry okara}} \tag{2}$$

Analysis of morphological structure and functional groups The morphological structures of raw and pretreated okara without or with ultrasound were verified by field emission scanning electron microscope (FE-SEM) (JEOL JSM-7800F, Japan), and their functional groups were analyzed by Fourier transform infrared spectroscopy (FTIR) (FT-730, Horiba, Kyoto, Japan) within the wave number range of 400−4000 cm^{-1}. Elemental analysis of various okara samples were performed with X-ray energy dispersive spectrometer (EDS). The ash content of okara sample was analyzed with EDS after carbonizing the sample in a heating plate at 300 °C for 90 min and then placing it in the ash furnace (PID-96T, RISEN, Taiwan) at 600 °C for 6 h.

Statistical analysis The experimental data were expressed as mean ± standard deviations from triplicate experiments. Statistical analysis was evaluated by one-way ANOVA with Duncan's multiple range test using IBM SPSS Statistics 20, and the significant difference was determined at $p < 0.05$.

The kinetic model In the past, several models for heterogeneous system have been proposed to describe the specific reactions, such as empirical models, models based on the Langmuir adsorption isotherm and the fractal Michaelis kinetics model (30−32). Due to the highly structured matrix of okara, the phenomena of enzymatic hydrolysis of okara are complex including the transport and reaction of enzymes within the network structure and the product inhibition, and the access as well as the adsorption of enzymes could influence the activity of enzymes. However, a simplified kinetic model that can be used to describe the enzymatic hydrolysis reactions would be advantageous for the design of the bioreactor. In this solid−liquid system, the enzymes should first diffuse from the liquid medium into the network structure of solid okara to conduct the reactions. During the transport processes, the mass-transfer resistance through the internal pores of okara and the adsorption of active enzymes on the inert materials result in the decrease of active enzymes. Such effects can be represented by the impeded reaction of the enzymes using the initial rate and deactivation coefficients. The hydrolysis reaction schemes using okara as the substrate and TRS as the product are

$$E + S \underset{k_{-1}}{\overset{k_1}{\rightleftarrows}} ES \tag{3}$$

$$ES \xrightarrow{k_2} E + P \tag{4}$$

$$E \xrightarrow{k_{dE}} IE \tag{5}$$

where S is okara substrate, E is the active enzymes, ES is the enzyme−substrate complex, P is the TRS product, and IE is the inactive enzymes, with k_1 and k_{-1} the forward and reverse reaction rate coefficients for Eq. 3, k_2 the rate constant for Eq. 4 and k_{dE} the deactivation coefficient for Eq. 5. The rate expressions for S, ES, E, and P are

$$\frac{d[S]}{dt} = -k_1[S][E] + k_{-1}[ES] \tag{6}$$

$$\frac{d[ES]}{dt} = k_1[S][E] - k_{-1}[ES] - k_2[ES] \quad (7)$$

$$\frac{d[E]}{dt} = -k_1[S][E] + k_{-1}[ES] + k_2[ES] - k_{dE}[E] \quad (8)$$

$$\frac{d[P]}{dt} = k_2[ES] \quad (9)$$

During the reaction, the concentration of ES can be assumed at quasi-steady-state, that is,

$$\frac{d[ES]}{dt} = k_1[S][E] - k_{-1}[ES] - k_2[ES] \cong 0 \quad (10)$$

Eq. 10 is rearranged to give $[ES] = [S][E]/k_M$ with $k_M = (k_{-1} + k_2)/k_1$. The expression of $[ES]$ is then substituted into Eqs. 8 and 9 to give

$$\frac{d[E]}{dt} = -k_{dE}[E] \quad (11)$$

$$\frac{d[P]}{dt} = \frac{k_2}{k_M}[S][E] \quad (12)$$

Eq. 11 is solved for $[E] = [E_0]$ at $t = 0$ to give

$$[E] = [E_0]\exp(-k_{dE}t) \quad (13)$$

From the material balance of S, ES and P, we have

$$[S_0] = [S] + [ES] + [P] \quad (14)$$

where $[S_0]$ is the initial concentration of S. Since $[ES]$ is usually greatly less than the sum of $[S]$ and $[P]$, Eq. 14 can be simplified to give

$$[S] = [S_0](1 - [P]/[S_0]) \quad (15)$$

By defining the yield of TRS as $Y = [P]/[S_0]$ and inserting the expression of $[E]/[E_0]$ from Eq. 13, Eq. 12 becomes

$$\frac{dY}{dt} = k_0([E]/[E_0])(1 - Y) = k_0 \exp(-k_{dE}t)(1 - Y) \quad (16)$$

for $Y = 0$ at $t = 0$ with $k_0 = k_2[E_0]/k_M$ being the initial observed rate constant.

Eq. 16 can be solved to get

$$-\ln(1 - Y) = (k_0/k_{dE})(1 - \exp(-k_{dE}t)) \quad (17)$$

The initial rate coefficients k_0 and the deactivation coefficient k_{dE} can be correlated from the plot of $-\ln(1 - Y)$ versus hydrolysis time by nonlinear regression method.

RESULTS AND DISCUSSION

Pretreatment of okara using choline acetate under ultrasound The components of Tainan No. 3 black soybean and raw okara were analyzed and compared for the contents of water, ash, crude protein, crude fat, and dietary fiber (Table S1). The raw okara (denoted as RBO) had the lower contents of crude protein (22.58 ± 0.08 %) and ash (3.57 ± 0.10 %) and higher contents of soluble fiber (3.57 ± 0.39 %) and non-soluble fiber (59.75 ± 1.68 %) than those black soybeans had, indicating that the okara could be a favorable source of dietary fiber supplement in food. For unfolding the highly structured fibers, the RBO powder was pretreated using [Ch][OAc], which was dissolved in water or acetate buffer solution, under ultrasound (40 kHz/300 W or 120 kHz/300 W) at 60 °C for 180 min. After pretreatment, the pretreated okara was recovered as precipitate and denoted as CABO40 and CABO120 for cases of RBO treated with [Ch][OAc] in acetate buffer solution under 40 kHz and 120 kHz of ultrasound, and CWBO40 and CWBO120 for cases of RBO treated with [Ch][OAc] in water under 40 kHz and 120 kHz of ultrasound, respectively.

The ratios of recovered okara and their crude protein and ash contents were measured for the okara after various pretreatment conditions (Table S2). The ratios of the recovered okara were 67 % for CWBO40, 78 % for CWBO120, 79 % for CABO40, and 79 % for CABO120, and the order of crude protein content was RBO (22.58 %) > CABO40 (20.73 %) ≈ CABO120 (20.52 %) > CWBO120 (18.89 %) > CWBO40 (17.10 %). This indicated that the most efficient pretreatment was CWBO40 with the significant reduction of crude protein to eliminate the interference for hydrolysis, but still retained a favorable protein content for use. Comparing the results of CWBO40 and CABO40, it also showed that the type of solvent used to prepare the [Ch][OAc] solution much affected the efficiency of pretreatment. This effect could be attributed to common-ion effect in the solution with the same acetate ion for [Ch][OAc] and acetate buffer solution. Concerning the effect of ultrasound in [Ch][OAc] pretreatment, the ultrasonic frequency had a significant effect for CWBO40 and CWBO120, but with insignificant effect for CABO40 and CABO120, displaying that the frequency 40 kHz was more intense than 120 kHz when the effective [Ch][OAc] aqueous solution was employed.

Effects of pretreatment and hydrolysis on the structure of okara Fig. 1 is the FE-SEM images showing the surface morphology of okara before and after pretreatment and hydrolysis with or without ultrasound. As shown in Fig. 1A, the morphology of RBO was the irregular block structure with rugged wave-like surface, making it difficult for enzymes to access and utilize the inner components of okara. After [Ch][OAc] pretreatment, the morphology of CWBO40 (Fig. 1B) showed that the original structure was unfolded and cracked into small pieces with many larger pores, facilitating the transport of enzymes into the network structure to reach the reaction sites more easily. The surface structure of RBO in 4 h of enzymatic hydrolysis using shaking at 120 rpm displayed that the original rugged wave-like surface of RBO was disappeared to become smooth outer surface after hydrolysis, as shown in Fig. 1C. This indicated that the enzymatic digestion mainly occurred around the outer region of RBO so as to smooth the reacted zone. Furthermore, the internal microstructure seemed not to be destroyed, and the transport of enzymes into the inner surface would be hindered. Fig. 1D shows the image of RBO in 4 h of enzymatic hydrolysis with ultrasound at 120 kHz. The microstructure of okara was crumbled and cracked with a relatively rough surface, when using 120 kHz of ultrasound to assist the hydrolysis reaction. With a much intense ultrasonic frequency 40 kHz for the hydrolysis of RBO, the seriously crumbled, cracked, and punched surface structure was observed, as shown in Fig. 1E. This exhibited that the contact area and space between enzymes and okara substrate was increased by ultrasonic irradiation. As shown in Fig. 1F, the network structure of okara had been greatly destroyed and eroded when using CWBO40 as the substrate after 4 h of hydrolysis reaction under 40 kHz of ultrasound, making internal surface area of okara largely exposed to reduce the mass-transfer resistance and enhance the hydrolysis efficiency.

The results of elemental analysis using EDS are shown in Table 1. It displayed that the pretreatment of okara by [Ch][OAc] was able to reduce the C/O mass ratio from 1.23 for RBO to 0.91 for CWBO40, 0.98 for CABO40, 0.98 for hydrolysis of CWBO40, and 0.98 for hydrolysis of CABO40. The approaching of C/O mass ratio to 0.9, which was the C/O mass ratio of cellulose, implied that the ratio of cellulose in the structure after pretreatment was enhanced. The EDS analysis demonstrated the effectiveness of bio-IL pretreatment on the modification of okara structure.

The FTIR analysis The functional groups before and after different pretreatment conditions for RBO, CWBO40, CWBO120, CABO40, and CABO120 were analyzed by FTIR. The results are shown in Fig. 2A. The spectral profiles of these materials at bands of 897, 1400, 1641, 1745, 2855, 2926, and 3436 cm^{-1} were rather similar but with various intensities, indicating that the pretreatment of okara with [Ch][OAc] either in acetate buffer solution or in water under ultrasound at 40 kHz or 120 kHz

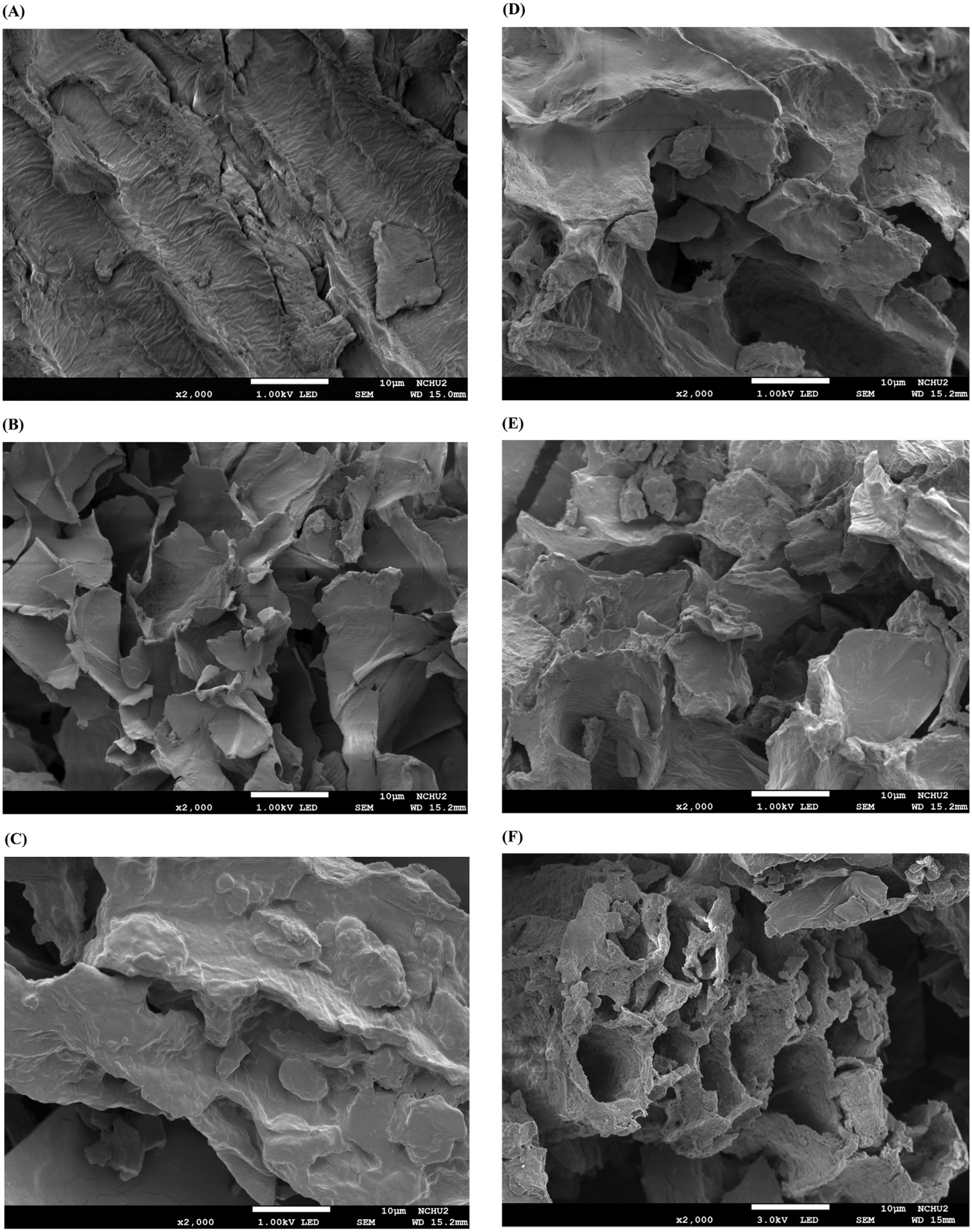

FIG. 1. FE-SEM images for okara before and after pretreatment and hydrolysis with or without ultrasound: (A) RBO; (B) CWBO40; (C) RBO after 4-h hydrolysis with shaking at 120 rpm; (D) RBO after 4-h hydrolysis with ultrasound at 120 kHz; (E) RBO after 4-h hydrolysis with ultrasound at 40 kHz; (F) CWBO40 after 4-h hydrolysis with ultrasound at 40 kHz. Scale bar: (A) 10 μm; (B) 10 μm; (C) 10 μm; (D) 10 μm; (E) 10 μm; (F) 10 μm.

TABLE 1. Elemental analysis of untreated and pretreated okara using EDS before and after 4 h of hydrolysis with or without ultrasound.

Sample	Hydrolysis conditions	C/O mass ratio	Element (%)[a]	
			C	O
RBO	–	1.23	55.15	44.85
CWBO40	–	0.91	47.76	52.24
CABO40	–	0.98	49.51	50.49
CWBO120	–	1.11	52.68	47.32
CABO120	–	1.21	54.40	44.97
RBO	Shaking, 120 rpm	1.31	56.80	43.20
RBO	Ultrasound, 40 kHz	1.17	47.22	40.28
RBO	Ultrasound, 120 kHz	1.42	53.35	37.70
CWBO40	Ultrasound, 40 kHz	0.98	46.14	47.27
CABO40	Ultrasound, 40 kHz	0.98	47.11	47.99

[a] Elements weight percentages were analyzed in selected sample area.

resulted in different degrees of structural changes but still having the similar functional groups. The broad bands of 3000–3650 cm^{-1} are O-H stretching of hydrogen attached to hydroxyl group (33). The band around 3436 cm^{-1} for CWBO40 was the most intensified among the tested samples, showing the largest ratio of O-H linkages enriched and exposed in the structure. The bands 2926 cm^{-1} and 2855 cm^{-1} were C-H stretching vibrations (34,35), and had the similar intensity for CWBO40, CWBO120, CABO40, and CABO120. The bands around 1745 cm^{-1} are the C=O stretching vibrations, including carboxylic acid or its ester (35). The intensities of bands around 1745 cm^{-1} for the pretreated okara were all slightly stronger than that for RBO, indicating the increase of carboxyl, ester and non-conjugated keto groups for pretreated okara. The bands around 1641 cm^{-1}, which were considered as peaks produced by conjugated carbonyl groups with double bonds, were similarly intensified for the tested samples. The bands around 1400 cm^{-1} are C-H stretching (34). The weak 1400 cm^{-1} band for CWBO40 was slightly stronger than that for others. The bands around 896 cm^{-1}, which were assigned to β-glycosides linkages between glucose in cellulose (33,36), were more intensified for CWBO40, CWBO120, CABO40, and CABO120 than that for RBO, showing the increase of available surface exposed.

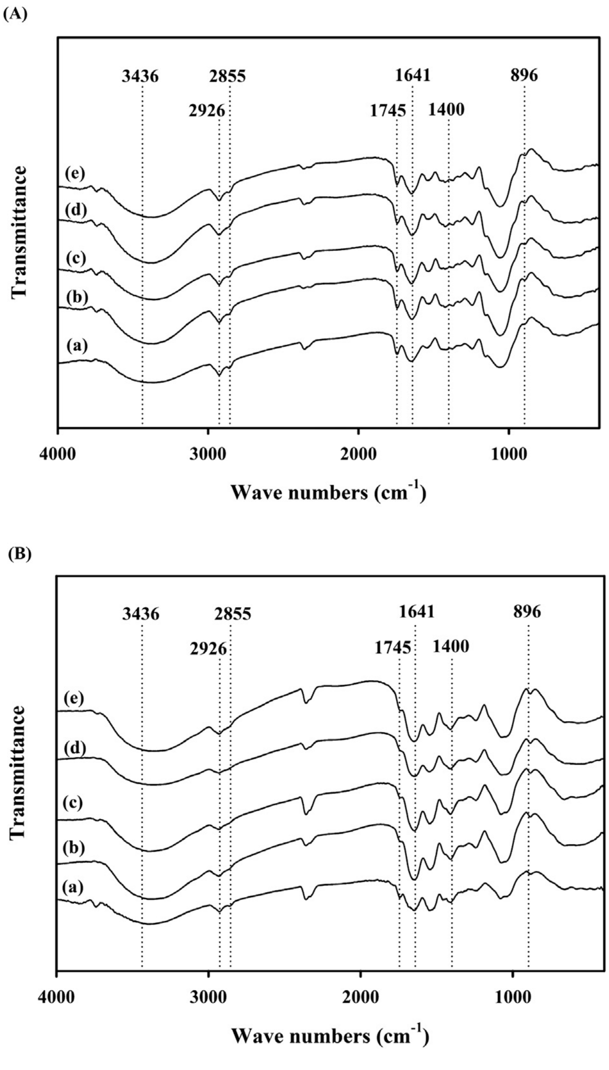

FIG. 2. FTIR spectra of okara: (A) with or without choline acetate pretreatment under different ultrasonic frequencies: a, RBO; b, CABO40; c, CABO120; d, CWBO40; e, CWBO120; (B) after 4 h of enzymatic hydrolysis: a, RBO with shaking at 120 rpm; b, RBO with ultrasound at 40 kHz; c, RBO with ultrasound at 120 kHz; d, CWBO40 with ultrasound at 40 kHz; e, CABO40 with ultrasound at 40 kHz.

The functional groups for RBO, CWBO40 and CABO40 in 4 h of enzymatic hydrolysis were analyzed, as shown in Fig. 2B. It was found that the intensities of bands around 3436 cm^{-1}, 1765 cm^{-1}, 1641 cm^{-1}, 1400 cm^{-1}, and 896 cm^{-1} for hydrolysis of RBO using shaking at 120 rpm (denoted as RBO-120R) were all significantly weaker than those for other samples, showing that the surface structure of RBO-120R was not opened up after hydrolysis. The result was consistent with the observation from FE-SEM image shown in Fig. 1C. The bands around 1745 cm^{-1} and 896 cm^{-1}, which were C=O stretching vibrations and β-glycosides linkages, showed more intensified for hydrolysis of CWBO40 with ultrasound at 40 kHz and CABO40 with ultrasound at 40 kHz than those for RBO with ultrasound at 40 kHz and 120 kHz. This implied that the valuable compounds having the functional groups of C=O or β-glycosides linkages from CWBO40 and CABO40 were enriched and exposed for use after enzymatic hydrolysis.

TRS production by enzymatic hydrolysis The enzymatic hydrolysis of okara (100 mg) to produce TRS with or without ultrasound and [Ch][OAc] pretreatment was performed using RBO, CABO40 and CWBO40 as the substrate at 50 °C for different reaction periods. Fig. 3A shows the comparison of TRS production of RBO hydrolysis using shaking at 120 rpm (denoted as RBO-120R) or ultrasound at 40 kHz (denoted as RBO-40KH) and 120 kHz (denoted as RBO-120KH). In 30 min of hydrolysis time, the difference in TRS productions between RBO-120R, RBO-40KH and RBO-120KH was insignificant. As the reactions proceeded over 60 min, the TRS production for RBO-40KH was significantly higher than those for RBO-120R and RBO-120KH. In 4 h of hydrolysis, the TRS production for RBO-40KH reached to 110.27 ± 5.44 mg/g-okara, which was 3.4 times of that for RBO-120R (32.18 ± 0.91 mg/g-okara) and greatly higher than 46.19 ± 2.51 mg/g-okara for RBO-120KH. The results confirmed the higher intensity of ultrasound at 40 kHz promoting the transport of enzyme into the network structure of RBO with greater efficiency, and consisted with the observation from FE-SEM images, EDS and FTIR analysis.

Fig. 3B displays the TRS productions for enzymatic hydrolysis under ultrasound at 40 kHz using the substrates RBO, CABO40, and CWBO40, and the substrates with the hydrolysis condition were denoted as RBO-40KH, CABO40-40KH, and CWBO40-40KH, respectively. In 30 min of reaction period, the TRS production for CWBO40-40KH was much higher than those for RBO-40KH and CABO40-40KH. However, in 4 h of hydrolysis time, the difference in TRS production for CABO40-40KH and CWBO40-40KH was statistically insignificant with TRS production of 162.38 ± 7.55 mg/g-okara for CABO40-40KH and 169.31 ± 14.99 mg/g-okara for CWBO40-40KH. These results were also consistent with the FTIR analysis in Fig. 2B. By the combination of [Ch][OAc] pretreatment

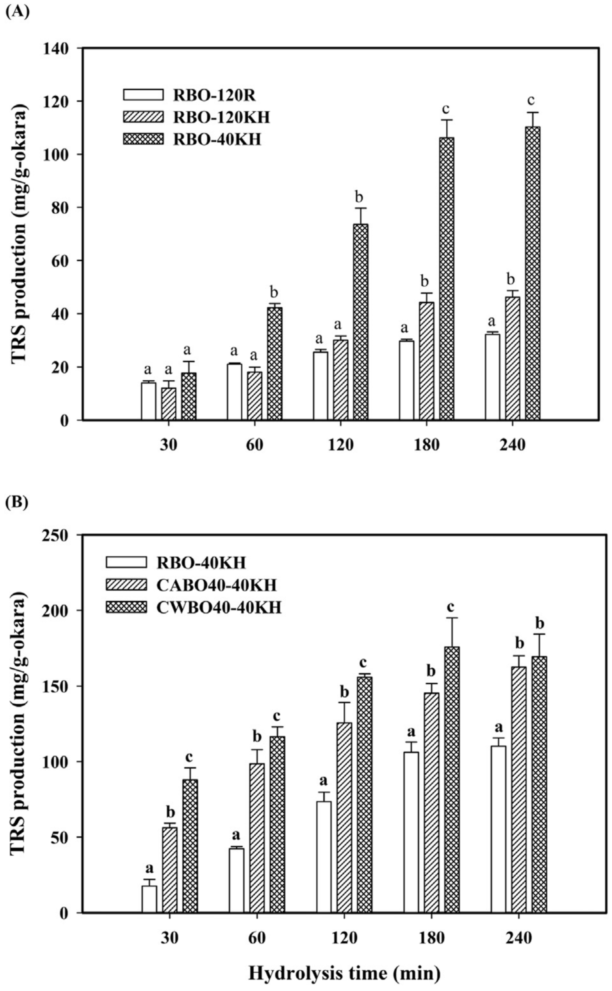

FIG. 3. Dependence of TRS production on hydrolysis time: (A) effect of ultrasonic frequency and shaking; (B) effect of choline acetate pretreatment. Data were expressed as mean ± standard deviations from triplicate experiments. Different superscript letters at the same group were significantly different ($p < 0.05$) by Duncan's test.

and ultrasound, the TRS production for CWBO40-40KH was about 5.2 times of that for RBO-120R.

Kinetic model for the enzymatic hydrolysis The kinetics for enzymatic hydrolysis under different hydrolysis conditions were analyzed using 100-mg untreated (RBO) or pretreated (CABO, CWBO) okara as the substrate. The TRS yields (Y, g-TRS/g-okara) were estimated from the TRS production at the reaction periods for each hydrolysis condition (Table S3). The initial rate coefficient k_0 and deactivation coefficient k_{dE} were correlated from experimental data using Eq. 17. The plots of $-\ln(1-Y)$ versus hydrolysis time for cases of RBO-120R, RBO-120KH, RBO-40KH, CABO40-40KH, and CWBO40-40KH are shown in Fig. 4. It was found that the satisfactory result was obtained for each case with the R-square of correlation greater than 0.96 (Table 2), demonstrating that the proposed kinetic model was successfully used to describe the enzymatic hydrolysis of this black soybean okara system.

The correlated initial rate coefficient k_0 and deactivation coefficient k_{dE} are displayed in Table 2. The order of k_0 (min^{-1}) were CWBO40-40KH > CABO40-40KH > RBO-40KH > RBO-120R > RBO-120KH. It showed that the initial rate coefficient of CWBO40-40KH was 6.56 times of that of RBO-120R, revealing the great enhancement of enzyme transport by bio-IL pretreatment. Besides, the largest impeded effect of enzyme was also presented for CWBO40-40KH with k_{dE} being 0.0193 min^{-1}. This implied that the impeded effect of enzyme from product inhibition was significant for the larger reaction rate. However, the high impeded effect for RBO-120R with 0.0177 min^{-1} of k_{dE} value was resulted from the limitation of enzyme transport that was obstructed by the highly structured network in the untreated okara.

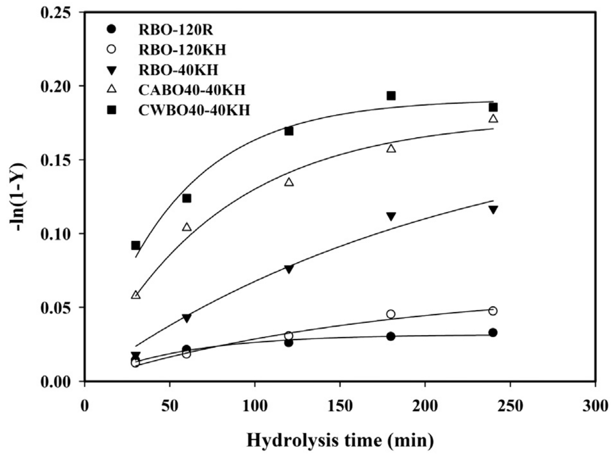

FIG. 4. Plot of −ln (1-Y) vs. hydrolysis time for the correlation of rate coefficients using 100-mg substrate. Symbols, experimental data; lines, model results.

TABLE 2. Correlated initial rate coefficient k_0 and deactivation coefficient k_{dE} for enzymatic hydrolysis using 100-mg untreated or pretreated okara as the substrate.

Substrate with hydrolysis conditions	10^3k_0 (min^{-1})[a]	10^2k_{dE} (min^{-1})[a]	R-square of correlation
RBO-120R	0.561	1.77	0.9648
RBO-120KH	0.380	0.59	0.9796
RBO-40KH	0.854	0.47	0.9797
CABO40-40KH	2.324	1.30	0.9821
CWBO40-40KH	3.688	1.93	0.9729

[a] The values of k_0 and k_{dE} were correlated from experimental data using Eq. 17.

Conclusion An effective method using bio-ionic pretreatment and ultrasound to promote the hydrolysis reaction of black soybean okara with cellulase was developed. The structure and the functional groups of untreated and pretreated okara were analyzed to verify the effect of pretreatment using choline acetate and ultrasound. The simplified kinetic model based on impeded reaction of enzymes was successfully applied to correlate the experimental data, and good fits of experimental data with the simulated values were obtained. The initial rate of reaction with ultrasound was higher than that without ultrasound. The kinetic model has the features of using limited kinetic parameters to describe the complex phenomena of deactivation behaviors of enzymes in a heterogeneous system. In summary, the utilization of black soybean okara can be effectively valorized by choline acetate pretreatment and enzymatic hydrolysis under ultrasound to produce fermentable sugars and modify the microstructural texture, so that the nutrients and digestion of okara can be enhanced for use in foods. The promising methodology developed in this study using the combination of non-toxic and biodegradable compound (choline acetate) and green technology (ultrasound) is not only friendly to the environment, but also advantageous to the simplification of the subsequent processing for the valorization of black soybean okara.

Supplementary data to this article can be found online at https://doi.org/10.1016/j.jbiosc.2018.12.007.

ACKNOWLEDGMENTS

The authors thank the Ministry of Science and Technology, Taiwan, R.O.C. for providing financial support for this research (project No. MOST 106-2221-E-030-018). The authors declare no conflict of interest.

References

1. **Lee, J. H. and Cho, K. M.:** Changes occurring in compositional components of black soybeans maintained at room temperature for different storage periods, Food Chem., **131**, 161–169 (2012).
2. **Yang, H. W., Hsu, C. K., and Yang, Y. F.:** Effect of thermal treatments on anti-nutritional factors and antioxidant capabilities in yellow soybeans and green-cotyledon small black soybeans, J. Sci. Food Agric., **94**, 1794–1801 (2014).
3. **Vong, W. C. and Liu, S. Q.:** Biovalorisation of okara (soybean residue) for food and nutrition, Trends Food Sci. Technol., **52**, 139–147 (2016).
4. **Nishinari, K.:** Texture and rheology in food and health, Food Sci. Technol. Res., **15**, 99–106 (2009).
5. **Jankowiak, L., Kantzas, N., Boom, R., and van der Goot, A. J.:** Isoflavone extraction from okara using water as extractant, Food Chem., **160**, 371–378 (2014).
6. **Katayama, M. and Wilson, L. A.:** Utilization of okara, a byproduct from soymilk production, through the development of soy-based snack food, J. Food Sci., **73**, 152–157 (2008).
7. **Vázquez, M. J., Alonso, J. L., Domínguez, H., and Parajó, J. C.:** Xylooligosaccharides: manufacture and applications, Trends Food Sci. Technol., **11**, 387–393 (2000).
8. **Villanueva-Suárez, M. J., Pérez-Cózar, M. L., and Redondo-Cuenca, A.:** Sequential extraction of polysaccharides from enzymatically hydrolyzed okara byproduct: physicochemical properties and in vitro fermentability, Food Chem., **141**, 1114–1119 (2013).
9. **Sun, F. and Chen, H.:** Enhanced enzymatic hydrolysis of wheat straw by aqueous glycerol pretreatment, Bioresour. Technol., **99**, 6156–6161 (2008).
10. **Wang, Z. and Feng, H.:** Fractal kinetic analysis of the enzymatic saccharification of cellulose under different conditions, Bioresour. Technol., **101**, 7995–8000 (2010).
11. **Kim, I. and Han, J. I.:** Optimization of alkaline pretreatment conditions for enhancing glucose yield of rice straw by response surface methodology, Biomass Bioenergy, **46**, 210–217 (2012).
12. **Kwiatkowska, B., Bennett, J., Akunna, J., Walker, G. M., and Bremner, D. H.:** Stimulation of bioprocesses by ultrasound, Biotechnol. Adv., **29**, 768–780 (2011).
13. **Lunelli, F. C., Sfalcin, P., Souza, M., Zimmermann, E., Prá, V. D., Foletto, E. L., Jahn, S. L., Kuhn, R. C., and Mazutti, M. A.:** Ultrasound-assisted enzymatic hydrolysis of sugarcane bagasse for the production of fermentable sugars, Biosyst. Eng., **124**, 24–28 (2014).
14. **Yang, C. Y., Sheih, I. C., and Fang, T. J.:** Fermentation of rice hull by *Aspergillus japonicus* under ultrasonic pretreatment, Ultrason. Sonochem., **19**, 687–691 (2012).
15. **Subhedar, P. B. and Gogate, P. R.:** Intensification of enzymatic hydrolysis of lignocellulose using ultrasound for efficient bioethanol production: a review, Ind. Eng. Chem. Res., **52**, 11816–11828 (2013).
16. **Yang, C. Y. and Fang, T. J.:** Kinetics of enzymatic hydrolysis of rice straw by the pretreatment with a bio-based basic ionic liquid under ultrasound, Process Biochem., **50**, 623–629 (2015).
17. **Vancov, T., Alston, A. S., Brown, T., and McIntosh, S.:** Use of ionic liquids in converting lignocellulosic material to biofuels, Renew. Energy, **45**, 1–6 (2012).
18. **Quijano, G., Couvert, A., and Amrane, A.:** Ionic liquids: applications and future trends in bioreactor technology, Bioresour. Technol., **101**, 8923–8930 (2010).
19. **Ninomiya, K., Ohta, A., Omote, S., Ogino, C., Takahashi, K., and Shimizu, N.:** Combined use of completely bio-derived cholinium ionic liquids and ultrasound irradiation for the pretreatment of lignocellulosic material to enhance enzymatic saccharification, Chem. Eng. J., **215–216**, 811–818 (2013).
20. **Blusztajn, J. K.:** Choline, a vital amine, Science, **281**, 794–795 (1998).
21. **Kasai, N., Murata, A., Inui, H., Sakamoto, T., and Kahn, R. T.:** Enzymatic high digestion of soybean milk residue (okara), J. Agric. Food Chem., **52**, 5709–5716 (2004).
22. **Asakawa, A., Oka, T., Sasaki, C., Asada, C., and Nakamura, Y.:** Cholinium ionic liquid/cosolvent pretreatment for enhancing enzymatic saccharification of sugarcane bagasse, Ind. Crop. Prod., **86**, 113–119 (2016).
23. **Ruß, C. and König, B.:** Low melting mixtures in organic synthesis – an alternative to ionic liquids? Green Chem., **14**, 2969–2982 (2012).
24. **Bureau of Standards, Metrology and Inspection:** Methods of test for moisture in food, CNS 5033 N6114. Bureau of Standards, Metrology and Inspection. Ministry of Economic Affairs, R.O.C., Taipei, Taiwan (1984).
25. **Bureau of Standards, Metrology and Inspection:** Method of test for ash in food, CNS 5034 N6115. Bureau of Standards, Metrology and Inspection. Ministry of Economic Affairs, R.O.C., Taipei, Taiwan (1984).
26. **Bureau of Standards, Metrology and Inspection:** Method of test for crude protein in food, CNS 5035 N6116. Bureau of Standards, Metrology and Inspection. Ministry of Economic Affairs, R.O.C., Taipei, Taiwan (1986).
27. **Bureau of Standards, Metrology and Inspection:** Methods of test for crude fat in food, CNS 5036 N6117. Bureau of Standards, Metrology and Inspection. Ministry of Economic Affairs, R.O.C., Taipei, Taiwan (1984).
28. **Horwitz, W. and Latimer, G. W.:** Total dietary fiber in foods, AOAC 985.29, in: Horwitz, W. and Latimer, G. W. (Eds.), Official methods of analysis of AOAC international, 18th ed. AOAC International, Gaithersburg, MD (2005).
29. **Yang, C. Y. and Fang, T. J.:** Combination of ultrasonic irradiation with ionic liquid pretreatment for enzymatic hydrolysis of rice straw, Bioresour. Technol., **164**, 198–202 (2014).
30. **Movagharnejad, K. and Sohrabi, M.:** A model for the rate of enzymatic hydrolysis of some cellulosic waste materials in heterogeneous solid–liquid systems, Biochem. Eng. J., **14**, 1–8 (2003).
31. **O'Dwyer, J. P., Zhu, L., Granda, C. B., Chang, V. S., and Holtzapple, M. T.:** Neural network prediction of biomass digestibility based on structural features, Biotechnol. Prog., **24**, 283–292 (2008).
32. **Flores-Sánchez, A., Flores-Tlacuahuac, A., and Pedraza-Segura, L. L.:** Model-based experimental design to estimate kinetic parameters of the enzymatic hydrolysis of lignocellulose, Ind. Eng. Chem. Res., **52**, 4834–4850 (2013).
33. **Ullah, I., Yin, T., Xiong, S., Zhang, J., Din, Z. U., and Zhang, M.:** Structural characteristics and physicochemical properties of okara (soybean residue) insoluble dietary fiber modified by high-energy wet media milling, LWT-Food Sci. Technol., **82**, 15–22 (2017).
34. **Zhou, T., Wang, H., Ji, S., Feng, H., and Wang, R.:** Synthesis of mesoporous carbon from okara and application as electrocatalyst support, Fuel Cell, **14**, 296–302 (2014).
35. **Gao, J., Si, C., and He, Y.:** Application of soybean residue (okara) as a low-cost adsorbent for reactive dye removal from aqueous solution, Desalin. Water Treat., **53**, 2266–2277 (2015).
36. **Lan, W., Liu, C. F., Yue, F. X., Sun, R. C., and Kennedy, J. F.:** Ultrasound-assisted dissolution of cellulose in ionic liquid, Carbohydr. Polym., **86**, 672–677 (2011).